MOLECULAR AND CELLULAR BIOLOGY, August 2001, p. 5190–5199 Vol. 21, No. 15
0270-7306/01/$04.00+0 DOI: 10.1128/MCB.21.15.5190–5199.2001

Identification of an Overlapping Binding Domain on Cdc20 for Mad2 and Anaphase-Promoting Complex: Model for Spindle Checkpoint Regulation

YONGKE ZHANG AND EMMA LEES*

Department of Oncology, DNAX Research Institute, Palo Alto, California 94304-1104

Received 8 December 2000/Returned for modification 29 January 2001/Accepted 24 April 2001

Activation of the anaphase-promoting complex (APC) is required for anaphase initiation and for exit from mitosis in mammalian cells. Cdc20, which specifically recognizes APC substrates involved in the metaphase-to-anaphase transition, plays a pivotal role in APC activation through direct interaction with the APC. The activation of the APC by Cdc20 is prevented by the interaction of Cdc20 with Mad2 when the spindle checkpoint is activated. Using deletion mutagenesis and peptide mapping, we have identified the sequences in Cdc20 that target it to Mad2 and the APC, respectively. These sequences are distinct but overlapping, providing a possible structural explanation for the internal modulation of the APC-Cdc20 complex by Mad2. In the course of these studies, a truncation mutant of Cdc20 (1–153) that constitutively binds Mad2 but fails to bind the APC was identified. Overexpression of this mutant induces the formation of multinucleated cells and increases their susceptibility to undergoing apoptosis when treated with microtubule-inhibiting drugs. Our experiments demonstrate that disruption of the Mad2-Cdc20 interaction perturbs the mitotic checkpoint, leading to premature activation of the APC, sensitizing the cells to the cytotoxic effects of microtubule-inhibiting drugs.

The growth of all organisms requires that the genome be accurately replicated and equally partitioned between two cellular progeny. The duplication of chromosomes, the separation of sister chromatids, and their segregation to opposite poles of the cell prior to cytokinesis are essential features of the cell cycle for the maintenance of genomic integrity. Chromosome duplication produces a pair of sister chromatids bound together by a multisubunit cohesin complex (25). To avoid missegregation, sister chromatids of each duplicated chromosome attach to the bipolar mitotic spindle through their kinetochores and align at the metaphase plate before their concomitant separation at anaphase. Cells possess regulatory mechanisms that delay sister chromatid separation and cytokinesis until the last chromosome has achieved bipolar attachment. Similar mechanisms block chromosome segregation and the onset of anaphase in the event of defective spindle assembly, as is induced by microtubule-inhibiting drugs such as nocodazole (26). This surveillance mechanism, termed the mitotic checkpoint, enables cells to repair the defect and thereby ensure the inheritance of an identical set of chromosomes in each daughter cell at mitosis (2, 27). Defects in the mitotic checkpoint can result in aneuploidy, which may contribute to genetic instability and consequently to the development of cancer (16).

Several key molecular components of the mitotic checkpoint have been identified through a combination of genetic studies of *Saccharomyces cerevisiae* and biochemical studies in *Xenopus laevis* egg extracts and mammalian cells. BUB (budding uninhibited by benzimidazole) family genes *Bub1, Bub2,* and *Bub3* (17) and MAD (mitotic arrest-deficient) family genes *Mad1*, *Mad2,* and *Mad3* (22); Pds1 (40); and Mps1 (15, 38) are all required for cell cycle arrest in response to inhibition of microtubule formation. Mad1, Mad2, Mad3, Bub1, and Bub3 were previously found to associate with kinetochores prior to chromosome alignment on the metaphase plate (5, 6, 19, 23, 32, 33), suggesting that these proteins are part of a conserved spindle checkpoint (Mad2 checkpoint) that monitors the completion of the spindle-kinetochore attachment (2). Bub2 is associated with the spindle pole body and participates in a distinct spindle position checkpoint (14) to block exit from mitosis (1, 13).

Entry into anaphase and exit from mitosis both depend on proteolysis of regulatory proteins (34). Sister chromatid separation depends on proteolysis of Pds1 (8), which binds to and inhibits Esp1, a protein required for sister chromatid separation (7, 35). Later, during late anaphase the inactivation of Cdc2 requires proteolysis of B-type cyclins. The degradation of all these proteins depends on a ubiquitin protein ligase called the anaphase-promoting complex (APC) or cyclosome (21, 31). The activity of APC is regulated by two related WD repeat-containing proteins, Cdc20 and Cdh1, which function as substrate-specific activators. Cdc20 promotes degradation of early substrates such as Pds1, whereas Cdh1 promotes degradation of late substrates such as cyclin B (28, 29, 36). The precise mechanism by which Cdc20 activates the APC remains unclear. Cdc20 does not appear to affect the phosphorylation state of the APC but may induce a structural change upon binding that promotes substrate-specific activation of the APC. At the molecular level, it has been proposed that the Mad2 checkpoint delays the metaphase-to-anaphase transition by inhibiting the activity of the APC through forming an inactive complex with Cdc20 and APC (12, 18). Anaphase is initiated only by the dissociation of Mad2 from the complex. While the nature of the checkpoint signal that inhibits APC activity is unknown, it is believed to stabilize the interactions between Mad2 and Cdc20.

In this study, we have undertaken a detailed structural anal-

* Corresponding author. Mailing address: DNAX Research Institute, 901 California Ave., Palo Alto, CA 94304. Phone: (650) 496-1257. Fax: (650) 496-1200. E-mail: emma.lees@dnax.org.

ysis of the interaction of Cdc20 with Mad2 and the APC to better understand at the molecular level how the APC is regulated. We demonstrate that the regions of Cdc20 that interact with these two components are distinct but overlapping, suggesting that Mad2 interaction may sterically hinder the interaction of Cdc20 with the APC. Using a Cdc20 mutant that can bind only to Mad2, we demonstrate that the selective disruption of the Mad2 mitotic checkpoint affects cell morphology and sensitivity to certain chemotherapeutic agents with microtubule-inhibiting activity.

MATERIALS AND METHODS

Cell culture and synchronization. Human lung cancer A549 cells were cultured in RPMI 1640 medium supplemented with 10% fetal calf serum; human embryonic kidney 293T cells were maintained in Dulbecco's modified Eagle's medium supplied with 10% fetal calf serum. Cells were arrested in metaphase with 400 ng of nocodazole (Sigma)/ml or 1 μM paclitaxel (Taxol; Sigma) for 18 h. For the double-thymidine block and release experiment, A549 cells were arrested for 14 h with 2 mM thymidine (Sigma), washed twice, released for 10 h in medium without thymidine, arrested again for 14 h with 2 mM thymidine, washed twice, and released into fresh medium. To arrest cells in mitosis without checkpoint activation, A549 cells were treated with 400 ng of nocodazole/ml and then released into fresh medium containing 10 μM MG-132 (Calbiochem). Samples were taken at the indicated time points.

Plasmid constructions and in vitro mutagenesis. The human Cdc20 cDNA was generated by PCR using a cDNA library isolated from A549 cells as the template and then subcloned into an *Eco*RI site of the pFlag-cytomegalovirus 2 (CMV-2) vector (Kodak, New Haven, Conn.). The C-terminally truncated mutants of Cdc20 cDNA were generated by adding a stop codon directly after amino acid 410, 310, 210, 153, or 101 using the QuikChange site-directed mutagenesis kit (Stratagene, La Jolla, Calif.). The N-terminally truncated mutants were generated by PCR, cloned into a pCR^{TOPO} vector (Invitrogen, San Diego, Calif.), and then transferred into Flag–CMV-2 vector. The wild-type (WT) Cdc20 and 1–153 mutant were also subcloned into green fluorescent protein (GFP) vector (Clontech). All cDNAs were confirmed by DNA sequencing.

Transfections. 293T and A549 cells were transiently transfected with 2 μg of the pFlag–CMV-2 vector or GFP empty vector or vectors containing WT Cdc20 and mutant cDNAs, using Effectant transfection reagent according to the manufacturer's instructions (Qiagen, Hilden, Germany). In some experiments, transfected A549 cells were treated with 0.4 μg of nocodazole/ml or 1 μM paclitaxel for an additional 18 h to induce multinucleated cells and apoptosis.

Cell cycle analyses. Cell cycle analysis was performed as previously described (41). Briefly, 10^6 cells were harvested and fixed with 70% ethanol followed by treatment with 1 mg of RNase/ml. The cells were stained with propidium iodide solution (3.2 mM sodium citrate, 50 mg of propidium iodide/ml, and 0.1% Triton X-100) for 30 min at 23°C. Then, the cells were resuspended and analyzed using a Becton Dickinson FACScan flow cytometer (Braintree, Mass.). The percentages of G_1, S, and G_2/M populations were calculated.

Morphological assessment of apoptosis. A549 cells transfected with GFP constructs were grown in the presence or absence of nocodazole or paclitaxel for 18 h. Cells were washed in phosphate-buffered saline (PBS) and then fixed in 3.7% paraformaldehyde for 15 min. The fixed cells were cytocentrifuged on slides, washed in PBS, and permeabilized with 0.5% Triton X-100. The cells were then stained with propidium iodide for 10 min, rinsed in PBS, and mounted under coverslips. The nuclear morphology of the GFP-positive cells was analyzed using confocal microscopy. More than 100 cells were counted to quantify apoptotic nuclei in three different experiments.

Western blotting and immunoprecipitations. For the 293T coimmunoprecipitation experiments, cells were lysed in lysis buffer containing 50 mM Tris-HCl, 300 mM NaCl, and 0.1% Nonidet P-40 plus protease inhibitors (complete EDTA-free tablets, protease inhibitor cocktail; Boehringer Mannheim). Immunoprecipitations were performed as previously described (41). Lysates were immunoprecipitated using Sepharose-conjugated M2 anti-Flag antibodies (Sigma). Lysates and immunoprecipitates were boiled, subjected to sodium dodecyl sulfate (SDS)–4 to 20% polyacrylamide gel electrophoresis (PAGE), and then electrotransferred onto nylon membranes (Immobilon-P; Millipore, Bradford, Mass.). Membranes were probed with one of the following antibodies: mouse monoclonal M5 anti-Flag antibody (Sigma), goat polyclonal antibodies against N-terminal and C-terminal Mad2 (Santa Cruz Biotechnology), and rabbit polyclonal anti-APC2 antibody (Neomarkers, Inc.). For the immunoprecipitations with synchronized A549 cells, cells were lysed as described above, and lysates were immunoprecipitated with goat polyclonal antibodies against N-terminal and C-terminal human Cdc20 (hCdc20; Santa Cruz Biotechnology). Membranes were immunoblotted with mouse monoclonal antibody to Mad2 (Transduction Laboratories) or rabbit polyclonal antibody to APC2 (Neomarkers, Inc.). Detection was then performed with enhanced chemiluminescence (ECL; Amersham).

Peptide inhibition assay. Peptides were synthesized by Research Genetics and dissolved in PBS. Cell extracts from 293T cells transfected with Flag-tagged Cdc20 were incubated with indicated peptides (100 μM) at 4°C for 2 h. The reaction mixtures were immunoprecipitated with goat polyclonal antibodies against N-terminal and C-terminal hCdc20 (Santa Cruz Biotechnology), and the immunoprecipitates were Western blotted with mouse anti-Mad2 monoclonal antibody or rabbit anti-APC2 polyclonal antibody (Neomarkers, Inc.).

Immunofluorescence. Cells on coverslips were fixed with 3.7% formaldehyde in PBS for 20 min, permeabilized with 0.5% Triton X-100 for 5 min at 23°C, and then blocked with 10% fetal bovine serum. For the detection of Flag-tagged Cdc20 and its mutant proteins, 293T cells were labeled for 1 h at room temperature with anti-Flag M5 monoclonal antibody at a 1:500 dilution. After cells were rinsed with PBS, secondary fluorescent antibody was applied at room temperature for 45 min. DNA was stained with 0.1 μg of propidium iodide/ml for 5 min before the coverslips were mounted with mounting medium. Cells were imaged by confocal microscopy (Leica TCS SP).

RESULTS

The binding of Cdc20 to Mad2 and the APC is cell cycle regulated. The activity of the APC is regulated by cell cycle and mitotic checkpoint signals. Activation of the APC requires the binding of the WD40 repeat-containing protein, Cdc20, which in turn is negatively regulated by its interaction with Mad2. To better understand how APC activation is coordinately regulated by Cdc20 and Mad2, we examined the association of Cdc20 with APC and Mad2, both as a function of the cell cycle and in response to checkpoint signals.

Human lung cancer A549 cells were synchronized at the G_1/S boundary by a double-thymidine block. The cells were then released into fresh medium to allow the cells to reenter the cell cycle, and fractions were collected at the indicated time points for analysis (Fig. 1A). As shown by Western blot analysis in Fig. 1C, the level of Cdc20 increased significantly as cells entered mitosis (4 to 6 h) and then decreased as cells entered the subsequent cell cycle. This pattern of expression mirrored that seen with the mitotically regulated cyclin B1. In contrast, the levels of Mad2 and APC2, a subunit of APC, were not changed during the cell cycle (Fig. 1C). To examine the composition of Cdc20-containing complexes during the cell cycle, we performed coimmunoprecipitations using an anti-Cdc20 antibody and then probed for the presence of Mad2 or APC2 by Western blotting. As shown in Fig. 1B, the association of Cdc20 with Mad2 and APC2 was induced in mitosis (4 to 6 h) concomitantly with the increase in total levels of Cdc20 protein. Mad2 association with Cdc20 was lost between 6 and 8 h after release, coincidentally with the decrease in cyclin B levels (Fig. 1C) signifying APC activation. The Cdc20-APC complex persisted through mitosis and declined as cells entered the next (G_1) phase. Similar results were obtained using mouse anti-Cdc27 monoclonal antibody, another APC subunit (APC3) (data not shown). Our data, together with previous reports (37), demonstrate a tightly cell cycle-regulated interaction of Cdc20 with Mad2 and APC.

The binding of Mad2 to Cdc20 is regulated by the mitotic checkpoint. We next investigated how the mitotic checkpoint regulates the binding of Cdc20 to Mad2 and APC. For these

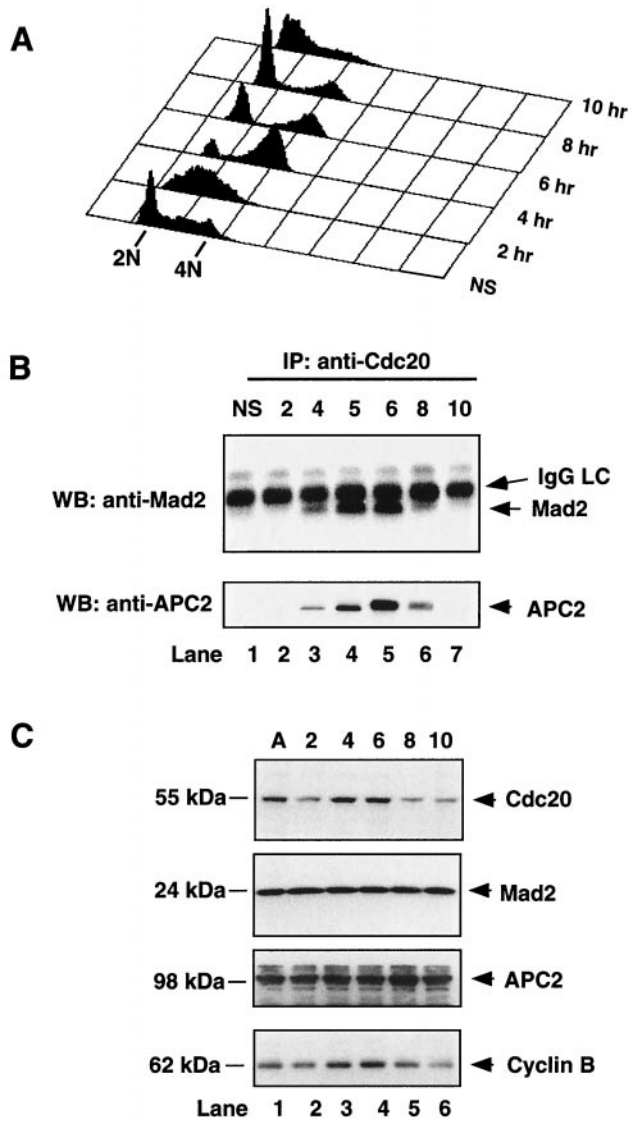

FIG. 1. Cell cycle-regulated association of Cdc20 with Mad2 and APC. A549 cells were synchronized at the G_1/S boundary by a double-thymidine block, released into fresh medium, and collected every hour after release. (A) The profile of DNA content of released cells was analyzed by fluorescence-activated cell sorting. (B) Cells collected at indicated time points (hours) were lysed, cell extracts were immunoprecipitated with goat anti-Cdc20 polyclonal antibody, and the immunoprecipitates were analyzed by Western blotting with mouse anti-Mad2 monoclonal antibody (upper panel) and rabbit anti-APC2 polyclonal antibody (lower panel). Asynchronous cells (lane 1) were included as a control. (C) The levels of Cdc20, Mad2, APC2, and cyclin B proteins at indicated time points (hours) were determined by Western blot analysis. NS, nonsynchronous; IP, immunoprecipitation; WB, Western blotting; IgG, immunoglobulin G; LC, light chain; A, asynchronous.

experiments, A549 cells were treated with nocodazole, a microtubule-inhibiting agent used to activate the mitotic checkpoint. After 18 h of treatment, cells arrested at prometaphase were collected by shake-off. The mitotic cells were then released from arrest by adding fresh medium, and fractions were taken at hourly intervals. Asynchronous cells and cells arrested at prometaphase by another microtubule-inhibiting agent, paclitaxel, were included as controls. As shown in Fig. 2B, the level of Cdc20 protein was increased in cells treated with nocodazole and paclitaxel and declined rapidly after the mitotically arrested cells were released. Unlike Cdc20, the protein levels of Mad2 and APC2 were not changed by either drug treatment. Coimmunoprecipitation experiments revealed that both Mad2 and APC were strongly associated with Cdc20 when the mitotic checkpoint was activated (Fig. 2A, lanes 3 and 7). When cells were released from nocodazole, Mad2 dissociated from Cdc20 very rapidly, while the APC-Cdc20 complex persisted somewhat (Fig. 2A, lanes 3 to 6).

Since nocodazole arrests cells in mitosis with an activated spindle checkpoint, the above experiment does not address whether the association of Mad2 with Cdc20 is simply a result of cells being in mitosis, as is the situation in yeast, or whether the association requires the spindle checkpoint to be activated. To address this issue, we took A549 cells arrested in mitosis by nocodazole and released them back into fresh medium containing the proteasome inhibitor MG-132. This treatment should allow cells to remain arrested in mitosis without activating the checkpoint. In contrast to cells released into fresh medium, cells released in the presence of MG-132 maintained high levels of Cdc20 and cyclin B (Fig. 2B, lanes 8 to 10). Interestingly, the binding of Mad2 to Cdc20 was still seen with MG-132-treated cells, although the levels appeared somewhat lower than those seen with checkpoint activation. In contrast, the levels of interaction between the APC and Cdc20 were increased in the presence of MG-132 (Fig. 2A, lanes 8 to 10). These data suggest that the binding of Mad2 and Cdc20 is induced in mitotic cells and is further enhanced upon checkpoint activation, presumably to counterbalance APC-Cdc20 interaction (compare lane 8 to lane 10 in Fig. 2A).

We next addressed whether the increased binding of Mad2 to Cdc20 observed upon checkpoint activation was simply due to an increase in Cdc20 protein levels in mitotic cells. A Flag-tagged Cdc20 construct was overexpressed in 293T cells, and then the cells were treated with nocodazole to activate the mitotic checkpoint. As shown in Fig. 2C, while nocodazole treatment did not affect the overall protein levels of Flag-Cdc20, the binding of Mad2 to Flag-Cdc20 was significantly increased. This result indicates that activation of the mitotic checkpoint modulates Mad2 to enhance its binding to Cdc20 and that this increased binding is independent of the protein level of Cdc20.

Our interpretation of the above experiments is contingent upon the existence of a ternary complex between Cdc20, Mad2, and APC. To demonstrate that this was indeed the case, we tested for the existence of a ternary complex in checkpoint-activated cells by immunodepleting Cdc20. Nocodazole-arrested A549 cells were immunodepleted of Cdc20 using an anti-Cdc20 antibody and then examined for the presence of Mad2-APC complexes by immunoprecipitation. As shown in Fig. 2D, following immunodepletion of Cdc20, we could no longer detect the binding of Mad2 to APC. As expected, depletion of Cdc20 also reduced the total levels of APC2 and, to a lesser extent, Mad2, since they are bound together in a complex. Control Western blotting to examine the levels of the cell cycle inhibitor p21 demonstrated the specificity of this immunodepletion. These results support previous reports that Cdc20, Mad2, and APC form a complex when the mitotic

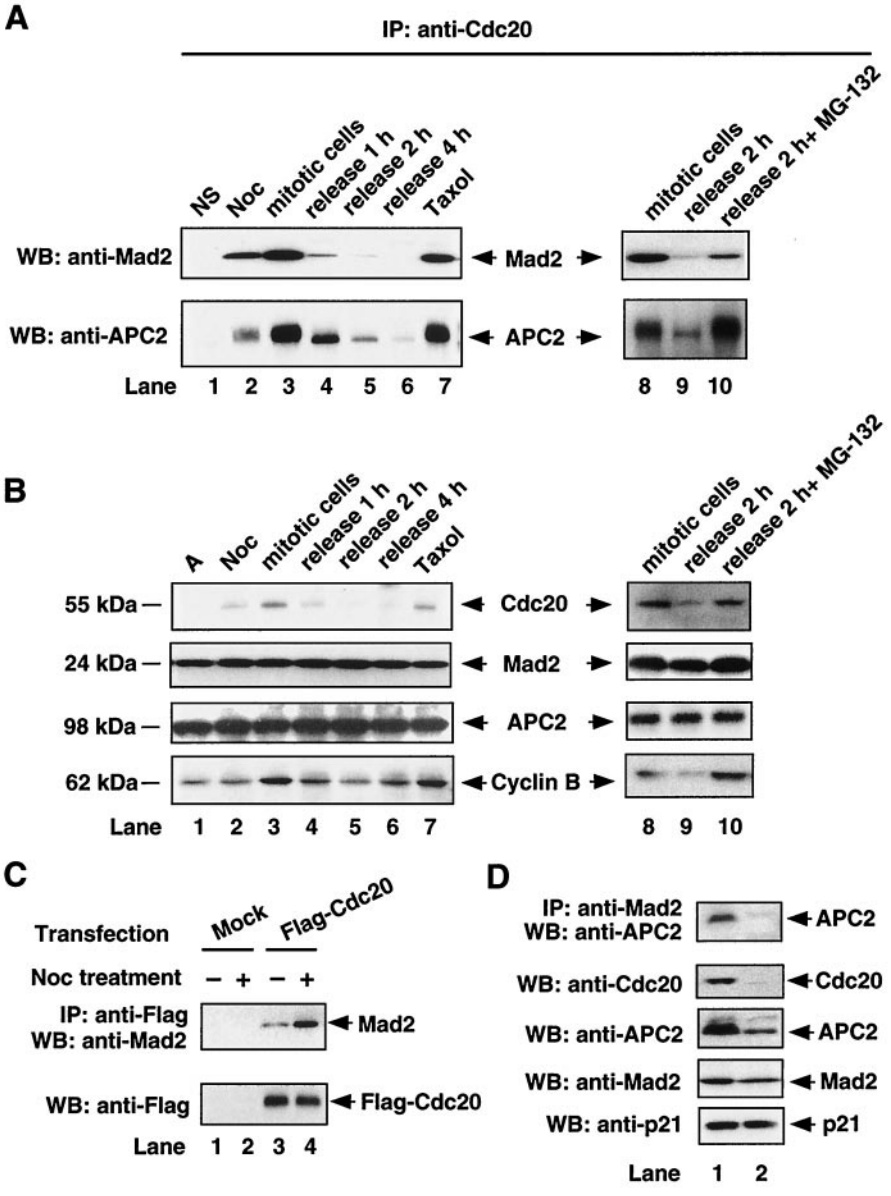

FIG. 2. Mitotic checkpoint-regulated association of Cdc20 with Mad2 and APC. (A) A549 cells were synchronized at prometaphase by nocodazole block. Mitotically arrested cells were collected by shake-off. Cells released into fresh medium were collected at indicated time points. To arrest cells in mitosis without activating the checkpoint, A549 cells were released from nocodazole into fresh medium containing 10 μM MG-132 (lane 10). Cell extracts (500 μg) were prepared at indicated time points and were immunoprecipitated with goat anti-Cdc20 polyclonal antibody, and the immunoprecipitates were analyzed by Western blotting with mouse anti-Mad2 monoclonal antibody (upper panel) and rabbit anti-APC2 polyclonal antibody (lower panel). Asynchronous cells (lane 1) and paclitaxel (lane 7) were included as controls. (B) The levels of Cdc20, Mad2, APC2, and cyclin B proteins at indicated time points and conditions were determined by Western blot analysis. (C) 293T cells were transfected with mock vector or Flag-tagged Cdc20 for 24 h. Transfected cells were treated with (+) or without (−) 0.4 μg of nocodazole/ml for 18 h. Cell extracts (1 mg) were immunoprecipitated with anti-Flag M2-conjugated agarose beads, and the immunoprecipitates were subjected to Western blot analysis with goat anti-Mad2 polyclonal antibody (upper panel). The level of Flag-tagged Cdc20 was determined by Western blotting with anti-Flag M5 monoclonal antibody (lower panel). (D) A549 cells were arrested in mitosis by nocodazole block, and cell extracts were immunoprecipitated with mouse anti-Mad2 monoclonal antibody either before (lane 1) or after (lane 2) immunodepletion with goat anti-Cdc20 polyclonal antibody. The immunoprecipitates were analyzed by Western blotting with rabbit anti-APC2 polyclonal antibody (upper panel). The amounts of Cdc20, APC2, Mad2, and p21 proteins in the supernatant before and after immunodepletion of Cdc20 were determined by Western blotting as indicated. IP, immunoprecipitation; NS, nonsynchronous; Noc, nocodazole; WB, Western blotting; A, asynchronous.

checkpoint is activated by spindle-disrupting agents such as nocodazole (12).

The Mad2 binding region of Cdc20 overlaps but is distinct from the APC binding region. To further investigate how Mad2 inhibits Cdc20 activation of APC, we mapped the region of Cdc20 involved in binding Mad2 and APC. A series of truncation mutants of Cdc20 were constructed (Fig. 3A) and expressed as Flag-tagged proteins in 293T cells. The Cdc20 C-

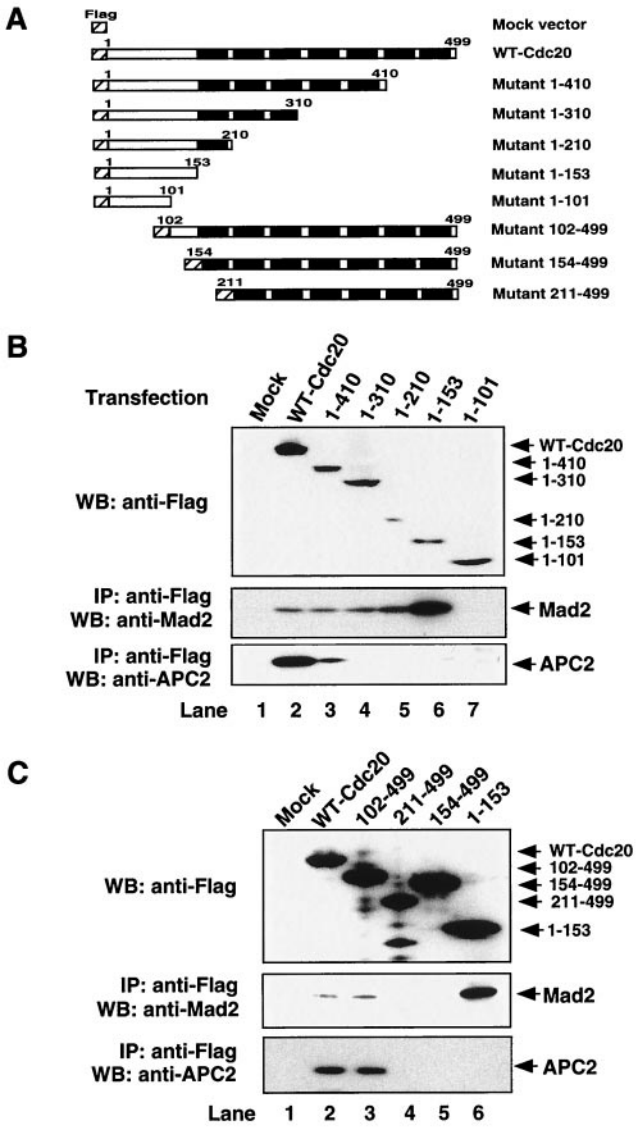

FIG. 3. The APC binding region of Cdc20 overlaps with but is distinct from the Mad2 binding region. (A) Schematic representation of Cdc20 deletion constructs. (B and C) 293T cells were transfected with equal amounts of indicated plasmids. After transfection for 24 h, cells were harvested, and expression of the corresponding WT and truncated mutant proteins was detected by Western blotting with anti-Flag M5 antibody (upper panels). Cell lysates were immunoprecipitated with anti-Flag M2 agarose beads. Precipitated proteins were separated by SDS-PAGE, transferred onto nylon membranes, and Western blotted with goat anti-Mad2 polyclonal antibody (middle panels) or rabbit anti-APC2 antibody (lower panels). WB, Western blotting; IP, immunoprecipitation.

terminal truncations 1–210, 1–310, and 1–410 were able to bind Mad2 as effectively as did the WT Cdc20. Surprisingly, we identified a short fragment, 1–153, which bound Mad2 much better than did either WT Cdc20 or other truncation mutants. The shortest truncation fragment of Cdc20 (1–101) failed to bind to Mad2 (Fig. 3B). An N-terminal truncation of Cdc20 (102–499) was able to bind Cdc20, while further deletions, 154–499 and 211–499, lost binding to Mad2 (Fig. 3C). These results indicate that a 52-amino-acid fragment of Cdc20 (102–153) contains the region of Cdc20 involved in Mad2 interaction. These results are consistent with the findings for yeast and for other mammalian systems (20, 24).

Because APC is a large multisubunit complex consisting of at least 11 proteins, we chose APC2 and APC3 (Cdc27) as representative subunits to map the interaction with Cdc20. Binding experiments demonstrated that the deletion of the C terminus of Cdc20 significantly decreased the binding of APC to Cdc20 (Fig. 3B, bottom panel). Unlike the Mad2 binding region, which is restricted to a small amino-terminal fragment, the APC binding region spanned a much longer stretch of Cdc20 (1–410), suggesting that the WD repeats in the carboxyl-terminal half may contribute to APC binding. Interestingly, deletion of the Mad2 binding region in Cdc20 (mutant 154–499) also disrupted the binding of APC to Cdc20 (Fig. 3C, bottom panel). Similar results were obtained using mouse anti-Cdc27 monoclonal antibody to detect APC3 (data not shown). These data suggest that the Mad2 binding region is also required for APC binding to Cdc20. Taken together, these results indicate that Mad2 and APC share an overlapping but distinct region of Cdc20 for interaction.

Cdc20 peptides spanning the Mad2 docking sequence inhibit the binding of Mad2 to Cdc20. To examine whether the Mad2 motif was sufficient for the Mad2-Cdc20 interaction, we synthesized several peptides spanning the Mad2 binding motif. These peptides were added as competitors into cell lysates from 293T cells transfected with Flag-tagged WT Cdc20 to inhibit endogenous Mad2 binding. We found that one peptide (amino acids 122 to 145) spanning the Mad2 binding motif specifically inhibited the binding of Mad2 to Cdc20 in a dose-dependent manner (Fig. 4B). In contrast, the peptide consisting of amino acids 102 to 121, which is also within the Mad2 binding motif, had no effects on the binding of Mad2 to Cdc20 (Fig. 4A, top panel). To examine whether the peptide 122–145 bound directly to Mad2, we incubated a biotin-conjugated peptide with 293T cell lysate and isolated complexes on streptavidin-agarose. As shown in Fig. 4C, the biotin-conjugated peptide 122–145, but not the control biotin-conjugated peptide, bound directly to Mad2. These results provide evidence that amino acids 122 to 145 of Cdc20 are necessary and sufficient for interaction with Mad2. This region of Cdc20 is highly conserved between species, as shown in Fig. 4D. Interestingly, all of the point mutations in yeast Cdc20 that inactivated the mitotic checkpoint are contained within this same region (highlighted in red). In other experiments, we also found that mutation of R132 to alanine in hCdc20 largely disrupted the binding of Cdc20 to Mad2 (data not shown).

We also examined the ability of these synthetic peptides to inhibit the interaction of APC with Cdc20. As shown in Fig. 4A, we found two peptides that were able to inhibit the binding of APC2 to Cdc20. One of them was the peptide 122–145, which also blocked Mad2 binding to Cdc20. These data support the deletion mutant analysis showing that Mad2 and APC share an overlapping region of Cdc20 for interaction. The inhibition of APC binding by peptide 166–178 indicates that the APC may also require other regions for effective binding to Cdc20.

Mapping the checkpoint activation domain of Cdc20. Our detailed mutational analysis suggested that there may be some level of internal competition between APC and Mad2 for in-

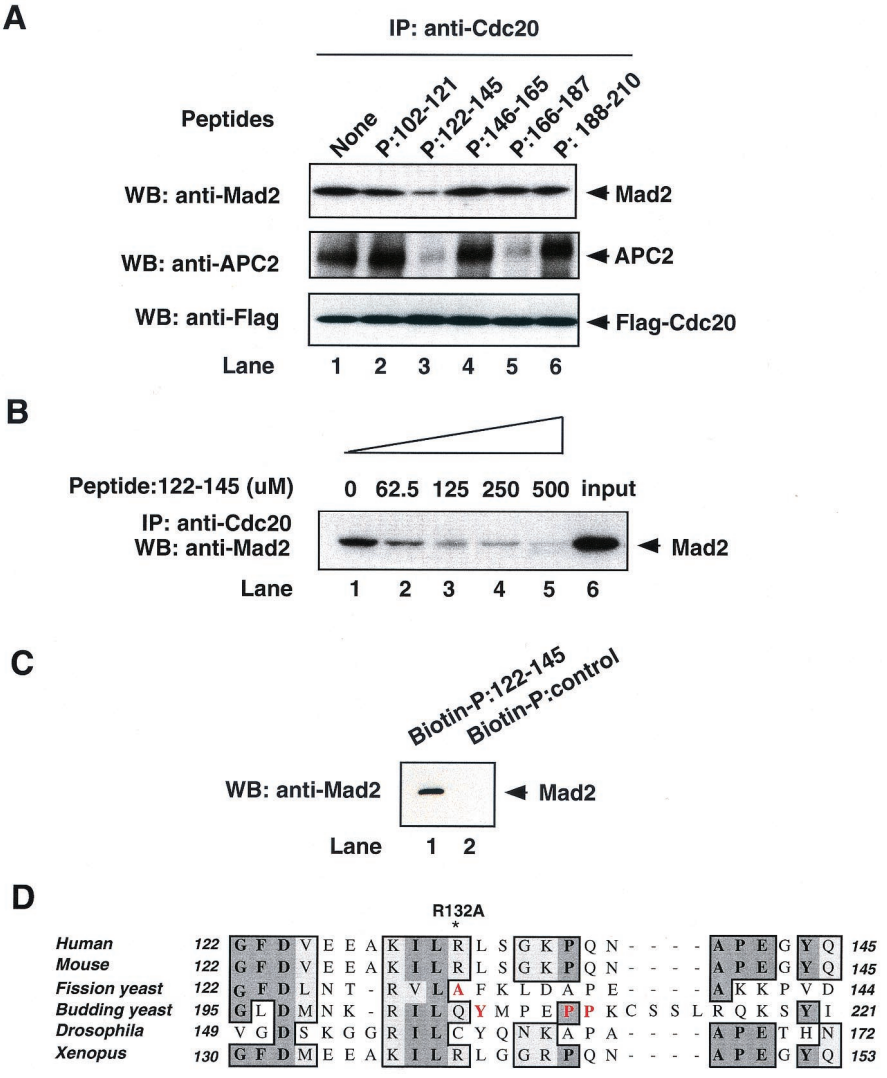

FIG. 4. Peptide inhibition of Mad2 and APC binding to Ccd20. (A) Extracts from 293T cells transfected with Flag-tagged WT Cdc20 were incubated with indicated peptides (100 μM) in vitro at 4°C for 2 h. Flag-Cdc20 protein was immunoprecipitated using anti-Flag M2 agarose beads and then immunoblotted with goat anti-Mad2 polyclonal antibody (upper panel), rabbit anti-APC2 polyclonal antibody (middle panel), or anti-Flag M5 antibody (lower panel). (B) Extracts from 293T cells transfected with Flag-tagged WT Cdc20 were incubated with indicated concentrations of peptide 122–145 in vitro at 4°C for 2 h. Flag-Cdc20 protein was immunoprecipitated using anti-Flag M2 agarose beads and then immunoblotted with goat anti-Mad2 polyclonal antibody. (C) Extracts from 293T cells were incubated with biotin-conjugated peptide 122–145 or control biotin-conjugated peptide for 2 h at 4°C. Biotin-conjugated peptides were pulled down with streptavidin beads, and then biotin-peptide-associated Mad2 was detected by Western blotting with goat anti-Mad2 polyclonal antibody. (D) Comparison of the amino acid sequence 122 to 145 of hCdc20 with the aligned sequences from mouse, fission yeast, budding yeast, *Drosophila melanogaster,* and *X. laevis*. The amino acid mutations in yeast that inactivate the mitotic checkpoint are shown in red. The R132A mutation in humans also reduces the binding of Cdc20 to Mad2 (unpublished data). The alignment was generated with ClustalW using MacVector 6.5 software. Identical and conserved amino acids are shown as shaded areas. IP, immunoprecipitation; WB, Western blotting.

teraction with Cdc20. Checkpoint signals may drive the equilibrium in favor of Mad2 binding or APC binding. In order to understand how the structure of Cdc20 affects checkpoint-activated modulation of Mad2 binding to Cdc20, we compared the abilities of WT Cdc20 and C-terminal deletion mutants of Cdc20 to interact with Mad2 in the presence of nocodazole. As shown in Fig. 5, nocodazole treatment significantly increased the binding of Mad2 to WT Cdc20, as shown previously (Fig. 2). In contrast, the binding of Cdc20 1–153, which has a higher basal level of Mad2 binding, was not further induced by checkpoint activation. Other Cdc20 truncations (1–210 and 1–310) had a low basal level of Mad2 binding that was strongly inducible with nocodazole treatment. These results suggest that mitotic checkpoint activation induces the interaction of Mad2 with WT Cdc20, potentially through affecting APC binding in some manner. Our results further suggest that residues 153 to 210 within Cdc20 may also interfere with Mad2 binding independently of the APC, since Cdc20 1–210 cannot bind APC, suggesting either steric hindrance or the possibility that other factors may bind within this region. Interestingly, a point mutation of residue 176 within this region increased the basal Mad2 binding (data not shown).

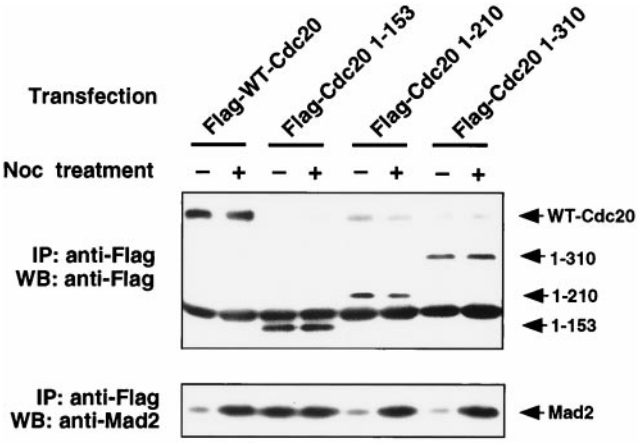

FIG. 5. Constitutive binding of 1–153 Cdc20 mutant to Mad2. 293T cells were transfected with equal amounts of indicated plasmids. After transfection for 24 h, cells were further treated with or without nocodazole for 18 h. Cells were harvested, and cell lysates were immunoprecipitated with anti-Flag agarose beads. Precipitated proteins were separated by SDS-PAGE, transferred onto nylon membranes, and Western blotted with goat anti-Mad2 polyclonal antibody (lower panel). The corresponding expression levels of WT and mutant proteins in transfected 293T cells were detected by Western blotting with anti-Flag M5 antibody (upper panel). Noc, nocodazole; IP, immunoprecipitation; WB, Western blotting.

Overexpression of Cdc20 1–153 disrupts the mitotic checkpoint and sensitizes cells to microtubule-inhibiting drugs. Since Cdc20 1–153 binds constitutively to Mad2 but does not interact with the APC, we looked at the ability of this mutant to disrupt the spindle checkpoint by sequestering Mad2, allowing premature activation of the APC. Surprisingly, we found that around 40% of Cdc20 1–153-transfected 293T cells formed aberrantly shaped multinucleated cells, as shown in Fig. 6A. The WT Cdc20-transfected cells were also able to form similar multinucleated cells but to a much lesser extent (Fig. 6A). Overexpression of the 1–310 mutant, which binds only to Mad2, also induced multinucleated and apoptotic cells, although to a lesser extent. Overexpression of the 1–410 mutant, which binds both APC and Mad2, had even more modest effects than did overexpression of the 1–310 mutant (data not shown). These data indicate that the presence of N-terminal sequences of the APC binding domain negates this effect on cell morphology. In contrast, the 1–101 and 211–499 mutants, which bind to neither Mad2 nor APC, were mislocalized to the perinuclear area and did not form any multinucleated cells (Fig. 6A). Similar observations were made using GFP fusion constructs expressing the WT Cdc20 and the 1–153 mutant in A549 cells (data not shown).

We next wished to determine whether the formation of multinucleated cells by the Cdc20 1–153 mutant was due to the disruption of the mitotic checkpoint by blocking Mad2 function. 293T cells were transfected with WT Cdc20 and 1–153, 1–101, and 211–499 mutants for 48 h and then treated with nocodazole for 18 h to see whether the mitotic checkpoint was still intact, by determination of the mitotic index. As shown in Fig. 6B, Cdc20 1–101- and 211–499-transfected cells were arrested in mitosis with a high mitotic index, whereas Cdc20 1–153-transfected cells had a low mitotic index and a high number of multinucleated cells and were accompanied by a rise in the apoptotic cells (Fig. 7A). These data indicated that the nocodazole exposure failed to arrest the Cdc20 1–153-transfected cells appropriately. Biochemical analysis demonstrated that overexpression of Cdc20 1–153 indeed blocked the endogenous Mad2 binding to Cdc20 in vivo, while the Cdc20 1–101 mutant had no effect (Fig. 6C).

There was an apparent increase in cell death when the Cdc20 1–153-tranfected 293T cells were treated with nocodazole. To further analyze this, we tested whether disruption of mitotic checkpoint with the Cdc20 1–153 mutant could increase the sensitivity of tumor cells to microtubule-inhibiting agents. As shown in Fig. 7, transfection of A549 cells with the Cdc20 1–153 mutant significantly increased the number of apoptotic cells in both nocodazole and paclitaxel treatments compared with mock GFP- or WT Cdc20-transfected cells. The difference in the morphologies of apoptotic and multinucleated cells is demonstrated in Fig. 7C. These data suggest that disruption of the mitotic checkpoint may sensitize tumor cells to the effects of microtubule-inhibiting drugs.

DISCUSSION

Cell cycle- and checkpoint-regulated binding of Mad2 to Cdc20. The separation of sister chromatids at the metaphase-anaphase transition depends on activation of the APC by Cdc20 (10, 30, 36). Because premature initiation of anaphase could lead to the formation of aneuploid daughter cells, the activation of the APC by Cdc20 has to be tightly controlled. Our results suggest that both Cdc20 turnover and the spindle assembly checkpoint contribute to the regulation of this event. By forming a complex with Cdc20 at a very early phase of mitosis, Mad2 may prevent premature activation of APC as Cdc20 protein begins to accumulate. We demonstrate that Mad2 binding to Cdc20 and, consequently, inhibition of APC activity are further enhanced by mitotic checkpoint activation. This could be due to modulation of Mad2 or Cdc20 by mitotic checkpoint signals. APC binding to Cdc20 is believed to be more dependent on the mitotic phosphorylation of APC core subunits than on the mitotic checkpoint signal, since Cdc20 can form binary complexes with APC without the Mad2 protein (37). Since ectopic overexpression of Cdc20 in cycling 293T cells is not sufficient to induce cyclin B proteolysis (data not shown), mitotic checkpoint control may be a rate-limiting step for the assembly of active APC-Cdc20 complexes, either through regulation of phosphorylation of APC or through activation of the Mad2 pathway. The proper timing of anaphase may therefore depend not only on the accumulation of Cdc20 between S phase and mitosis but also on the completion of spindle assembly to inactivate the mitotic checkpoint.

Proposed binding model. Through deletion mutant and peptide competition analysis, we have revealed that Mad2 binds to a small fragment of Cdc20, amino acids 122 to 145. Dominant mutations of Cdc20 in yeast have helped define the Mad2 binding motif to within this same small region (18, 20). Interestingly, we found that the APC binding region overlaps with the Mad2 binding motif. This predicts that Mad2 may compete with APC for the shared binding region in Cdc20. For APC binding, a larger region of Cdc20 is required, including the WD repeat at the C terminus. Since a ternary complex can exist, it

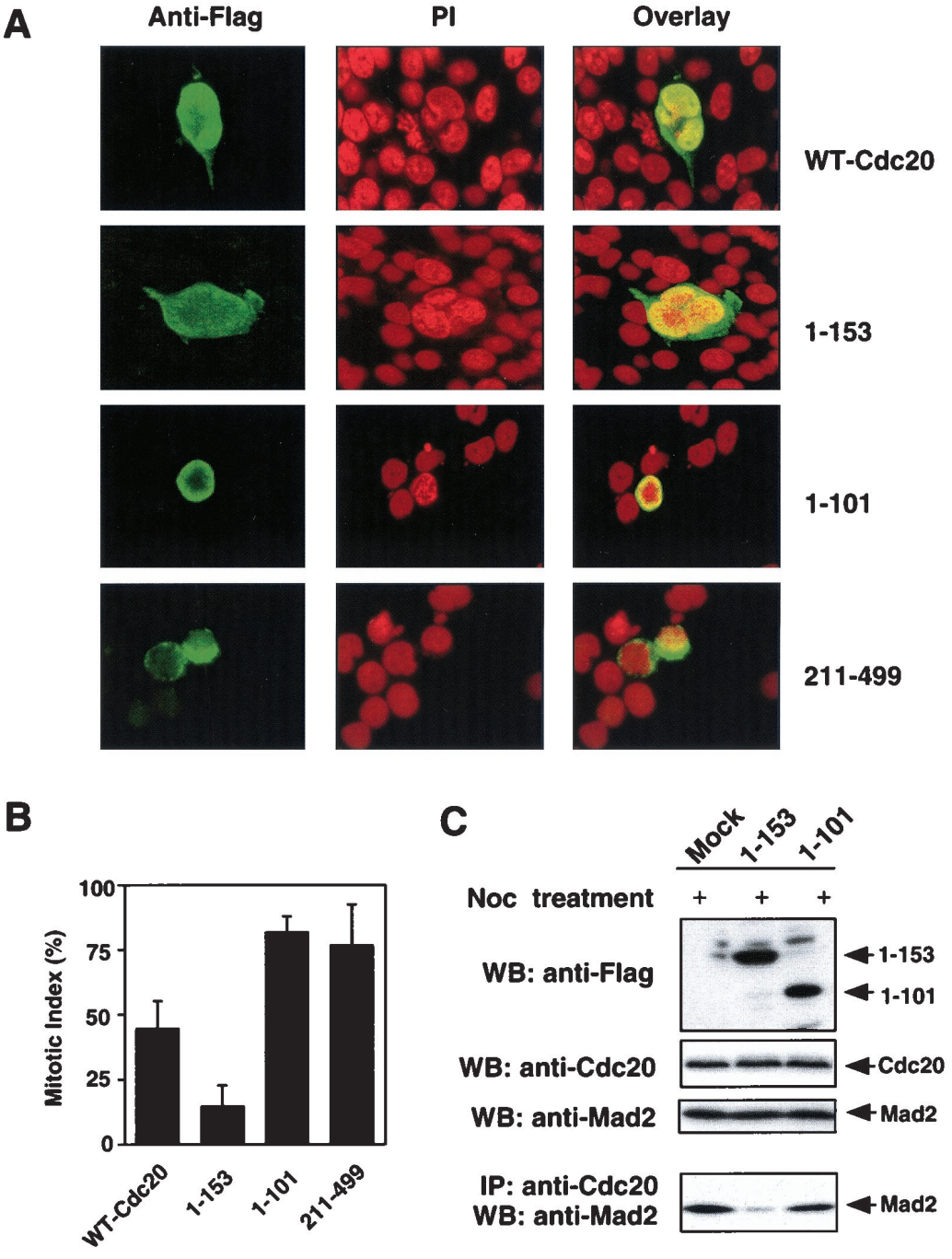

FIG. 6. Phenotype of 293T cells overexpressing WT Cdc20 and mutants. (A) 293T cells were transfected with pFlag-CMV vectors encoding WT Cdc20, 1–153 Cdc20, 1–101 Cdc20, or 211–499 Cdc20. After transfection for 48 h, the transfected cells were detected by immunofluorescence using anti-Flag M5 antibody. DNA was stained with propidium iodide. (B) The above transfected 293T cells were further treated with nocodazole for 18 h. The mitotic index was analyzed by fluorescence microscopy using anti-Flag M5 antibody for positive cells and propidium iodide for chromosome DNA. The shaded bars and error bars represent the means and standard deviations, respectively, from at least two independent assessments of 100 cells each in a single experiment; similar results were obtained in two independent experiments. (C) 293T cells were transfected with pFlag-CMV vectors encoding 1–153 Cdc20, 1–101 Cdc20, or vector control for 48 h and were further treated with nocodazole for 18 h. The levels of the corresponding truncated mutant protein, endogenous Cdc20, and Mad2 were detected by Western blotting with anti-Flag M5 antibody, goat anti-Cdc20 polyclonal antibody, and mouse anti-Mad2 monoclonal antibody. Cell lysates were immunoprecipitated with goat anti-Cdc20 polyclonal antibody. Precipitated proteins were separated by SDS-PAGE, transferred onto nylon membranes, and Western blotted with mouse anti-Mad2 monoclonal antibody. PI, propidium iodide; Noc, nocodazole; WB, Western blotting; IP, immunoprecipitation.

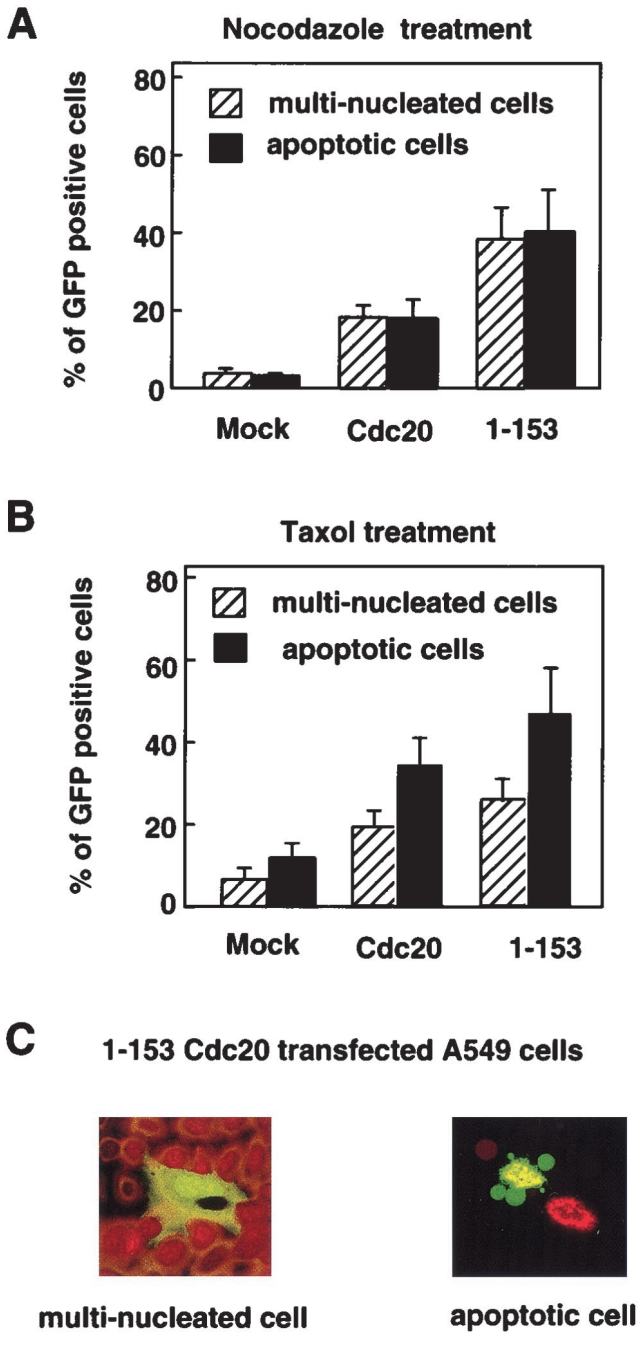

FIG. 7. A549 cells were transfected with pEGFP vector encoding WT Cdc20 or 1–153 Cdc20 mutant for 24 h and were further treated with nocodazole (A) or paclitaxel (B) for 18 h. GFP fusion constructs were directly visualized by autofluorescence. Multinucleated cells with aberrantly shaped nuclei and apoptotic cells with nuclear condensation and fragmentation were determined by counting 100 GFP-positive cells visualized with propidium iodide staining. The data show the averages and standard deviations derived from three experiments. (C) Representative morphology of paclitaxel-treated A549 cells transfected with 1–153 Cdc20.

is possible that the presence of all three proteins allows only a weak interaction with Cdc20 that is strengthened in favor of Mad2 in response to spindle damage or weakened in response to cell cycle progression, as demonstrated in Fig. 2. These signals may be mitotic kinases acting upon either Cdc20 or Mad2. One such kinase may be BubR1, which has also been shown previously to interact with Cdc20 (39). This complex is detected only in the presence of nocodazole and interestingly was absent when cells were released in the presence of proteasome inhibitors (unpublished data), suggesting a tight link with checkpoint activation. The equilibrium between Mad2 and APC binding is also disrupted in the case of the Cdc20 1–153 mutant, which can no longer bind APC. In this case, Mad2 binding to Cdc20 1–153 is constitutively high and, interestingly, no longer inducible upon checkpoint activation. The constitutive interaction of Cdc20 1–153 with Mad2 could be due to loss of APC binding or the loss of an interaction with an accessory molecule that promotes the formation or activity of Cdc20-APC complexes. Whether Mad2 inhibits Cdc20 through its blocking access of Cdc20 to ubiquitination substrates remains to be determined.

Functional study of mutant 1–153. Overexpression of Cdc20 1–153 induced the formation of multinucleated cells. Treatment of these cells with nocodazole failed to induce an arrest, suggesting that the spindle checkpoint had been disrupted. This phenotype has been seen in some previous studies where the mitotic checkpoint was disrupted by inactivation of upstream genes such as those encoding murine Bub1 and human BubR1 and Mad1 (3, 4, 33). Compared to single cells, the cyclin B level was high in most multinucleated cells, suggesting that the multinucleated cells may be caused by dysregulation of mitotic exit or cytokinesis (data not shown). The multinucleated phenotype may be related to the Bub2-mediated checkpoint, which regulates mitotic exit by inhibiting cyclin B degradation. This hypothesis is supported by yeast studies which showed that the nocodazole-induced cell cycle arrest of a *mad2* mutant is totally abolished by deletion of Bub2 but not by that of Bub1, Mad1, or Mad3 (1). The Bub2 pathway may detect spindle defects occurring after anaphase onset as a result of Mad2 checkpoint deficiency, since Bub2-dependent pathways have a common function to inhibit cytokinesis or mitotic exit until they reach a defined position. Recent identification of the mammalian homologue of Bub2 protein GAPCenA may help us to investigate the Bub2 checkpoint pathway in mammalian cells (9). Interestingly, our data demonstrate that cells with a disrupted Mad2-dependent checkpoint have a heightened sensitivity to both paclitaxel and nocodazole, and many underwent apoptosis in the presence of these drugs. Thus, it would appear that the checkpoint may have two outputs. The first is an apoptotic response when cells attempt to exit mitosis while the mitotic checkpoint is still active, as shown by our data with overexpression of Cdc20 1–153, as well as with the Mad2-knockout mice (11). The second response is a cell cycle arrest, as seen with the inhibition of Cdc20 through inactivation of mitotic checkpoint, such as dominant-negative Bub1 protein (33).

Our results support the hypothesis that disruption of the Mad2-dependent mitotic checkpoint sensitizes tumor cells to microtubule-inhibiting agents. Consistent with our data, a breast cancer cell line, T47D, which has a low expression of Mad2, showed increased sensitivity to microtubule-disrupting drugs (23). The cause of apoptosis under these conditions remains to be determined, but dysregulation of cyclin B levels could be an important factor. These results suggest that spe-

cific inhibition of mitotic checkpoint controls could make chemotherapy more effective and selective, as tumors often have a higher mitotic index than does the surrounding normal tissue.

ACKNOWLEDGMENTS

We are grateful to W. Korver, A. Walter, D. Parry, J. Johnston, and B. Amati for discussions and comments on the manuscript.

DNAX Research Institute is owned by Schering-Plough Corporation.

REFERENCES

1. **Alexandru, G., W. Zachariae, A. Schleiffer, and K. Nasmyth.** 1999. Sister chromatid separation and chromosome re-duplication are regulated by different mechanisms in response to spindle damage. EMBO J. **18:**2707–2721.
2. **Amon, A.** 1999. The spindle checkpoint. Curr. Opin. Genet. Dev. **9:**69–75.
3. **Chan, G. K., S. A. Jablonski, V. Sudakin, J. C. Hittle, and T. J. Yen.** 1999. Human BUBR1 is a mitotic checkpoint kinase that monitors CENP-E functions at kinetochores and binds the cyclosome/APC. J. Cell Biol. **146:**941–954.
4. **Chen, R. H., D. M. Brady, D. Smith, A. W. Murray, and K. G. Hardwick.** 1999. The spindle checkpoint of budding yeast depends on a tight complex between the Mad1 and Mad2 proteins. Mol. Biol. Cell **10:**2607–2618.
5. **Chen, R. H., A. Shevchenko, M. Mann, and A. W. Murray.** 1998. Spindle checkpoint protein Xmad1 recruits Xmad2 to unattached kinetochores. J. Cell Biol. **143:**283–295.
6. **Chen, R. H., J. C. Waters, E. D. Salmon, and A. W. Murray.** 1996. Association of spindle assembly checkpoint component XMAD2 with unattached kinetochores. Science **274:**242–246.
7. **Ciosk, R., W. Zachariae, C. Michaelis, A. Shevchenko, M. Mann, and K. Nasmyth.** 1998. An ESP1/PDS1 complex regulates loss of sister chromatid cohesion at the metaphase to anaphase transition in yeast. Cell **93:**1067–1076.
8. **Cohen-Fix, O., J. M. Peters, M. W. Kirschner, and D. Koshland.** 1996. Anaphase initiation in Saccharomyces cerevisiae is controlled by the APC-dependent degradation of the anaphase inhibitor Pds1p. Genes Dev. **10:**3081–3093.
9. **Cuif, M. H., F. Possmayer, H. Zander, N. Bordes, F. Jollivet, A. Couedel-Courteille, I. Janoueix-Lerosey, G. Langsley, M. Bornens, and B. Goud.** 1999. Characterization of GAPCenA, a GTPase activating protein for Rab6, part of which associates with the centrosome. EMBO J. **18:**1772–1782.
10. **Dawson, I. A., S. Roth, and S. Artavanis-Tsakonas.** 1995. The Drosophila cell cycle gene fizzy is required for normal degradation of cyclins A and B during mitosis and has homology to the CDC20 gene of Saccharomyces cerevisiae. J. Cell Biol. **129:**725–737.
11. **Dobles, M., V. Liberal, M. Scott, R. Benezra, and P. Sorger.** 2000. Chromosome missegregation and apoptosis in mice lacking the mitotic checkpoint protein Mad2. Cell **101:**635–645.
12. **Fang, G., H. Yu, and M. W. Kirschner.** 1998. The checkpoint protein MAD2 and the mitotic regulator CDC20 form a ternary complex with the anaphase-promoting complex to control anaphase initiation. Genes Dev. **12:**1871–1883.
13. **Fesquet, D., P. J. Fitzpatrick, A. L. Johnson, K. M. Kramer, J. H. Toyn, and L. H. Johnston.** 1999. A Bub2p-dependent spindle checkpoint pathway regulates the Dbf2p kinase in budding yeast. EMBO J. **18:**2424–2434.
14. **Fraschini, R., E. Formenti, G. Lucchini, and S. Piatti.** 1999. Budding yeast Bub2 is localized at spindle pole bodies and activates the mitotic checkpoint via a different pathway from Mad2. J. Cell Biol. **145:**979–991.
15. **Hardwick, K. G., E. Weiss, F. C. Luca, M. Winey, and A. W. Murray.** 1996. Activation of the budding yeast spindle assembly checkpoint without mitotic spindle disruption. Science **273:**953–956.
16. **Hartwell, L.** 1992. Defects in a cell cycle checkpoint may be responsible for the genomic instability of cancer cells. Cell **71:**543–546.
17. **Hoyt, M. A., L. Totis, and B. T. Roberts.** 1991. S. cerevisiae genes required for cell cycle arrest in response to loss of microtubule function. Cell **66:**507–517.
18. **Hwang, L. H., L. F. Lau, D. L. Smith, C. A. Mistrot, K. G. Hardwick, E. S. Hwang, A. Amon, and A. W. Murray.** 1998. Budding yeast Cdc20: a target of the spindle checkpoint. Science **279:**1041–1044.
19. **Jin, D. Y., F. Spencer, and K. T. Jeang.** 1998. Human T cell leukemia virus type 1 oncoprotein Tax targets the human mitotic checkpoint protein MAD1. Cell **93:**81–91.
20. **Kim, S. H., D. P. Lin, S. Matsumoto, A. Kitazono, and T. Matsumoto.** 1998. Fission yeast Slp1: an effector of the Mad2-dependent spindle. Science **279:**1045–1047.
21. **King, R. W., J. M. Peters, S. Tugendreich, M. Rolfe, P. Hieter, and M. W. Kirschner.** 1995. A 20S complex containing CDC27 and CDC16 catalyzes the mitosis-specific conjugation of ubiquitin to cyclin B. Cell **81:**279–288.
22. **Li, R., and A. W. Murray.** 1991. Feedback control of mitosis in budding yeast. Cell **66:**519–531.
23. **Li, Y., and R. Benezra.** 1996. Identification of a human mitotic checkpoint gene: hsMAD2. Science **274:**246–248.
24. **Luo, X., G. Fang, M. Coldiron, Y. Lin, H. Yu, M. W. Kirschner, and G. Wagner.** 2000. Structure of the Mad2 spindle assembly checkpoint protein and its interaction with Cdc20. Nat. Struct. Biol. **7:**224–229.
25. **Nasmyth, K., J. M. Peters, and F. Uhlmann.** 2000. Splitting the chromosome: cutting the ties that bind sister chromatids. Science **288:**1379–1385.
26. **Nicklas, R. B.** 1997. How cells get the right chromosomes. Science **275:**632–637.
27. **Rudner, A. D., and A. W. Murray.** 1996. The spindle assembly checkpoint. Curr. Opin. Cell Biol. **8:**773–780.
28. **Schwab, M., A. S. Lutum, and W. Seufert.** 1997. Yeast Hct1 is a regulator of Clb2 cyclin proteolysis. Cell **90:**683–693.
29. **Shirayama, M., A. Toth, M. Galova, and K. Nasmyth.** 1999. APC(Cdc20) promotes exit from mitosis by destroying the anaphase inhibitor Pds1 and cyclin Clb5. Nature **402:**203–207.
30. **Shirayama, M., W. Zachariae, R. Ciosk, and K. Nasmyth.** 1998. The Polo-like kinase Cdc5p and the WD-repeat protein Cdc20p/fizzy are regulators and substrates of the anaphase promoting complex in Saccharomyces cerevisiae. EMBO J. **17:**1336–1349.
31. **Sudakin, V., D. Ganoth, A. Dahan, H. Heller, J. Hershko, F. C. Luca, J. V. Ruderman, and A. Hershko.** 1995. The cyclosome, a large complex containing cyclin-selective ubiquitin ligase activity, targets cyclins for destruction at the end of mitosis. Mol. Biol. Cell **6:**185–197.
32. **Taylor, S. S., E. Ha, and F. McKeon.** 1998. The human homologue of Bub3 is required for kinetochore localization of Bub1 and a Mad3/Bub1-related protein kinase. J. Cell Biol. **142:**1–11.
33. **Taylor, S. S., and F. McKeon.** 1997. Kinetochore localization of murine Bub1 is required for normal mitotic timing and checkpoint response to spindle damage. Cell **89:**727–735.
34. **Townsley, F. M., and J. V. Ruderman.** 1998. Proteolytic ratchets that control progression through mitosis. Trends Cell Biol. **8:**238–244.
35. **Uhlmann, F., F. Lottspeich, and K. Nasmyth.** 1999. Sister-chromatid separation at anaphase onset is promoted by cleavage of the cohesin subunit Scc1. Nature **400:**37–42.
36. **Visintin, R., S. Prinz, and A. Amon.** 1997. CDC20 and CDH1: a family of substrate-specific activators of APC-dependent proteolysis. Science **278:**460–463.
37. **Wassmann, K., and R. Benezra.** 1998. Mad2 transiently associates with an APC/p55Cdc complex during mitosis. Proc. Natl. Acad. Sci. USA **95:**11193–11198.
38. **Weiss, E., and M. Winey.** 1996. The Saccharomyces cerevisiae spindle pole body duplication gene MPS1 is part of a mitotic checkpoint. J. Cell Biol. **132:**111–123.
39. **Wu, H., Z. Lan, W. Li, S. Wu, J. Weinstein, K. Sakamoto, and W. Dai.** 2000. P55cdc/Hcdc20 is associated with BUBR1 and may be a downstream target of the spindle checkpoint kinase. Oncogene **19:**4557–4562.
40. **Yamamoto, A., V. Guacci, and D. Koshland.** 1996. Pds1p, an inhibitor of anaphase in budding yeast, plays a critical role in the APC and checkpoint pathway(s). J. Cell Biol. **133:**99–110.
41. **Zhang, Y., N. Fujita, and T. Tsuruo.** 1999. p21Waf1/Cip1 acts in synergy with bcl-2 to confer multidrug resistance in a camptothecin-selected human lung-cancer cell line. Int. J. Cancer **83:**790–797.